**Supplementary materials for manuscript**

# NOVEL METABOLIC FEATURES IN ACINETOBACTER BAYLYI ADP1 REVEALED BY A MULTIOMICS APPROACH

[1-3]Lucille Stuani, [1-3]Christophe Lechaplais, [1-4]Aaro V. Salminen, [1-3]Béatrice Ségurens, [1-3]Maxime Durot, [1-3]Vanina Castelli, [1-3]Agnès Pinet, [1-3]Karine Labadie, [1-3]Stéphane Cruveiller, [1-3]Jean Weissenbach, [1-3]Véronique de Berardinis, [1-3]Marcel Salanoubat, [1-3]Alain Perret*

[1]Direction des Sciences du Vivant, Commissariat à l'Energie Atomique et aux Energies Alternatives (CEA), Institut de Génomique, Evry, France.
[2]CNRS-UMR8030, Evry, France.
[3]Université d'Evry Val d'Essonne, Evry, France.
[4]Tampere University of Technology, Department of Chemistry and Bioengineering, Korkeakoulunkatu 10, 33720 Tampere, Finland

*aperret@genoscope.cns.fr; Tel: 33-1-60-87-45-90; Fax: 33-1-60-87-25-14

**Check list**

**Protocol S-1** Dehydroquinate synthesis

**Table S-1** Primers used for the construction of the deletion mutants

**Table S-2** AMP, ADP and ATP calibration curves in positive ionization mode with AEC calculations using RAW and XCMS data

**Table S-3** Summary of the RNA sequencing coverage data

**Table S-4** Expression profiles of log phase cultures of *Acinetobacter baylyi* ADP1 grown on succinate and quinate

**Table S-5** List and details about the 114 commercial metabolites used as standards

**Table S-6** Full set of metabolites detected in Acinetobacter baylyi ADP1 metabolome

**Table S-7** Identified metabolites in Acinetobacter baylyi ADP1 metabolome

**Figure S-12** Tandem mass spectrum for N-acetyl aspartic acid in negative ionization mode

**Figure S-13** Tandem mass spectrum for mono-methyl hydrogen succinic acid in negative ionization mode

**Figure S-14** Tandem mass spectrum for trigonelline in positive ionization mode

**Protocol S-1 Dehydroquinate synthesis**

ADP1 was grown in 150 ml of quinate-containing growth medium to induce quinate dehydrogenase production. Cells were harvested after centrifugation (30 min, 2500 g, 4°C). The cell pellet was suspended in 1 ml of 50 mM phosphate buffer; pH 8.0, containing 1 µl Lysonase (Novagen) and 10% (v/v) BugBuster (Novagen) and let for 20 min at room temperature under vigorous shaking, and centrifuged (30 min, 20 000 g, 4°C). The supernatant was recovered and assayed for quinate dehydrogenase activity according to Adachi *et al*. (Adachi et al. 2003). For the use of enzymatically produced dehydroquinate as a reference compound for metabolite identification, 11 µg of lysate proteins were incubated in 1 ml of 50 mM phosphate buffer; pH 8.0, containing 10 mM quinate for 60 min. Proteins were discarded using 3K centrifugal PES filters, and 200 µl of the mixture were added to 800 µl 80/20 acetonitrile/ammonium carbonate pH 9.9 for LC/MS analysis.

REFERENCE:

Adachi, O., et al. (2003). Purification and characterization of membrane-bound quinoprotein quinate dehydrogenase. Biosci Biotechnol Biochem 67, 2115-23

**Table S-1 Primers used for the construction of the deletion mutants**

| Primers | Sequences |
|---|---|
| Primers for the integration cassette | |
| Primer_1: | 5'-CCCAGCCTCCAATTCAAATCATAAAAAAT-3' |
| Primer_2: | 5'-CCAGCTCCGCATGCTTAGAAAAACTCATCG-3' |
| | |
| Primers for ΔACIAD1738 | |
| Primer_3: | 5'-TCGCTATAAATAATCGCTACGC-3' |
| Primer_4: | 5'-TTTTTATGATTTGAATTGGAGGCTGGGTCAACGTGCTCCAATTTC-3' |
| Primer_5: | 5'-CGATGAGTTTTTCTAAGCATGCGGAGCTGGTTCAACATGATTTAGGAACATTC-3' |
| Primer_6: | 5'-TAATACCCAATGTTTCACCAGC-3' |
| Primer_7: | 5'-ATCAAATTGGTCAGTCCATCAC-3' |
| primer_8: | 5'-GACCAAATTGGATTACATCACC-3' |
| | |
| Primers for ΔACIAD3353 | |
| Primer_3: | 5'-TGAGCTTCAGTTACAGCGTACC-3' |
| Primer_4: | 5'-TTTTTATGATTTGAATTGGAGGCTGGGTCTGAGGATTTAGCTGACTACC-3' |
| Primer_5: | 5'-CGATGAGTTTTTCTAAGCATGCGGAGCTGGAAGCAAGTCATACATAAGGTG-3' |
| Primer_6: | 5'-CATCAGAAGTACGAAAAACCTC-3' |
| Primer_7: | 5'-GACGGGATTTAGTGTTAGCAAC-3' |
| Primer_8: | 5'-CGCTGCACTGTCACTCGTAAAG-3' |

**Table S-3 Summary of the RNA sequencing coverage data**

| Statistics | Carbon source | |
|---|---|---|
| | Succinate | quinate |
| Total number of reads | 25,986,330 ± 5,046,266 | 29,840,121 ± 5,467,425 |
| Total reads (Gb) | 1.97 | 2.27 |
| Genome coverage (fold) | 503 | 580 |
| Mapped reads (%) | 97.46 ± 0.16 | 97.31 ± 1.13 |
| Unique matches (%) | 90.22 ± 0.71 | 82.40 ± 1.03 |
| Total unmapped reads (%) | 2.54 ± 0.16 | 2.69 ± 1.13 |
| Reads mapped on rRNA (%) | 6.06 ± 1.00 | 13.91 ± 0.40 |

**Table S-5 Names, molecular mass and retention time of the 114 commercial metabolites detected by LC/MS.** Each compound is injected at 50 µM. Isoprene, butanal, deoxyribose, histidinol, pyridoxamine-5-phosphate, thyramine, and diaminopropane could not be detected on at least one column.

| Metabolite name | Molecular mass | Retention time on C18 (min) | Retention time on ZIC-pHILIC (min) |
|---|---|---|---|
| Propanoate | 74.0368 | 1.22 | 4.47 |
| Glycine | 75.032 | 0.96 | 11.28 |
| Pyruvate | 88.016 | 1.02 | 4.24 |
| Butanoic acid | 88.0524 | 1.83 | 3.58 |
| Alanine | 89.04767 | 0.96 | 10.63 |
| Lactate | 90.0317 | 0.99 | 5.16 |
| Acetoacetate | 102.0317 | 1.06 | 10.77 |
| Gamma-Aminobutyrate (GABA) | 103.0633 | 0.97 | 11.17 |
| Hydroxypyruvate | 104.011 | 0.9 | 6.89 |
| Serine | 105.0426 | 0.94 | 11.3 |
| D-Glyceric acid | 106.0266 | 0.94 | 7.51 |
| Catechol | 110.0368 | 4.6 | 3.78 |
| Isocytosine | 111.0433 | 1.38 | 7.2 |
| Cytosine | 111.0433 | 1.18 | 7.74 |
| Uracil | 112.0273 | 1.35 | 5.36 |
| Proline | 115.0633 | 1.07 | 9.1 |
| Fumarate | 116.011 | 0.9 | 11.16 |
| 3-Methyl-2-Oxobutyrate | 116.0473 | 1.4 | 7.75 |
| Betaine | 117.07897 | 1 | 7.8 |
| Valine | 117.079 | 1.21 | 8.91 |
| Succinate | 118.0266 | 1.12 | 10.5 |
| Threonine | 119.0582 | 0.99 | 10.8 |
| Homoserine | 119.0582 | 0.96 | 10.78 |
| Mercaptopyruvate | 119.9881 | 1.07 | 11.54 |
| Cysteine | 121.0197 | 1.17 | 11.94 |
| Nicotinamide (Niacinamide) | 122.048 | 2.66 | 4.36 |
| Nicotinate | 123.032 | 1.74 | 3.87 |
| Taurine | 125.0147 | 0.95 | 10.31 |
| Thymine | 126.0429 | 2.62 | 4.31 |
| 4-Methyloxovalerate | 130.0629 | 2.63 | 2.72 |
| 2-Ketohexanoate | 130.06299 | 2.67 | 2.69 |
| (Iso)Leucine | 131.0946 | 1.8 | 7.95 |
| Oxaloacetate | 132.0059 | 0.91 | 14.15 |
| Ornithine | 132.08987 | 0.91 | 18.84 |
| Aspartate | 133.0375 | 0.92 | 10.35 |
| Malate | 134.0215 | 0.92 | 11.19 |
| Adenine | 135.0545 | 1.67 | 6.27 |
| Hypoxanthine | 136.0385 | 1.62 | 6.77 |
| p-Aminobenzoate | 137.0477 | 1.72 | 6.19 |
| Anthranilic acid | 137.0477 | 3.13 | 8.24 |
| Trigonelline | 137.0477 | 1.05 | 8.23 |
| 2-Ketoglutarate | 146.0215 | 0.97 | 16.44 |
| Glutamine | 146.0691 | 1.35 | 10.68 |

| | | | |
|---|---|---|---|
| Lysine | 146.1055 | 0.92 | 20.54 |
| Glutamate | 147.0532 | 0.93 | 10.07 |
| Methionine | 149.051 | 1.4 | 8.08 |
| Guanine | 151.0494 | 1.59 | 8.67 |
| Xanthine | 152.0334 | 1.6 | 7.44 |
| 2.3-Dihydroxybenzoic acid | 154.0266 | 1.49 | 4.18 |
| Protocatechuate | 154.0266 | 1.89 | 8.94 |
| Histidine | 155.0695 | 1.18 | 12.84 |
| Orotic acid | 156.0171 | 1.04 | 5.87 |
| Allantoin | 158.0439 | 1.02 | 9.62 |
| Phenylpyruvate | 164.0473 | 1.64 | 9.29 |
| 7-Methylguanine | 165.0651 | 2.51 | 6.5 |
| Phenylalanine | 165.079 | 3.82 | 6.88 |
| Phosphoenolpyruvate | 167.9824 | 0.91 | 12.62 |
| Pyridoxamine | 168.0899 | 1.91 | 8.74 |
| Pyridoxine | 169.0739 | 2.02 | 4.84 |
| n-Capric acid | 172.1463 | 10.92 | 2.38 |
| Aconitate | 174.0164 | 0.9 | 12.69 |
| Shikimate | 174.0528 | 0.95 | 9.47 |
| N-Acetylornithine | 174.1004 | 1.05 | 11.05 |
| Arginine | 174.1117 | 0.96 | 22.02 |
| Citrulline | 175.0957 | 1.01 | 11.52 |
| Glucosamine | 179.0794 | 0.96 | 11.33 |
| Hydroxyphenylpyruvate | 180.0423 | 1.91 | 11.41 |
| myo-Inositol | 180.0634 | 0.99 | 12.28 |
| Tyrosine | 181.0739 | 1.57 | 9.28 |
| 3-Phosphoglycerate | 185.9929 | 0.85 | 12.24 |
| Citrate | 192.027 | 0.92 | 13.08 |
| Tryptophan | 204.0899 | 4.52 | 8.32 |
| Pantothenic acid | 219.1107 | 1.93 | 4.5 |
| Cystathionine | 222.0674 | 0.95 | 12.81 |
| Deoxycytidine | 227.0906 | 2.03 | 7.17 |
| Deoxyuridine | 228.0746 | 2.65 | 5.06 |
| Thymidine | 242.0903 | 4.16 | 4.22 |
| Cytidine | 243.0855 | 1.55 | 8.37 |
| Uridine | 244.0695 | 1.96 | 6.52 |
| Biotin | 244.0882 | 3.09 | 4.74 |
| Deoxyadenosine | 251.1018 | 4.5 | 5.02 |
| Deoxyinosine | 252.0859 | 3.4 | 6.29 |
| Glucosamine-6-phosphate | 259.0457 | 0.87 | 11.51 |
| Glucose-6-phosphate | 260.0297 | 0.92 | 11.91 |
| Thiamine | 265.1123 | 1.49 | 20.78 |
| Adenosine | 267.0968 | 4.36 | 5.84 |
| Inosine | 268.0808 | 3.13 | 7.49 |
| Guanosine | 283.0917 | 3.31 | 8.96 |
| Xanthosine | 284.0757 | 2.17 | 7.94 |
| dCMP | 307.0569 | 1.03 | 10.26 |
| Reduced Glutathione | 307.0838 | 1.01 | 13.28 |
| CMP | 323.0519 | 0.94 | 11.08 |
| UMP | 324.0359 | 0.98 | 10.5 |
| Cyclic AMP | 329.0525 | 4.17 | 5.38 |
| AMP | 347.0631 | 1.26 | 9.38 |
| dGMP | 347.0631 | 1.22 | 10.88 |
| IMP | 348.0471 | 1.15 | 10.8 |

| | | | |
|---|---|---|---|
| GMP | 363.058 | 1.11 | 11.71 |
| Riboflavin | 376.1383 | 6.31 | 5.43 |
| S-Adenosyl-L-methionine | 398.1372 | 1.18 | 12.83 |
| CDP | 403.0182 | 0.85 | 12.22 |
| ADP | 427.0294 | 1.05 | 10.77 |
| dGDP | 427.0294 | 1.01 | 12.07 |
| Folate | 441.1397 | 5.31 | 11.78 |
| CTP | 482.9845 | 0.84 | 13.23 |
| ATP | 506.9957 | 0.99 | 11.84 |
| dGTP | 506.9957 | 0.88 | 13.08 |
| GTP | 522.9907 | 0.86 | 13.9 |
| Oxidized Glutathione | 612.152 | 0.98 | 12.12 |
| NAD | 664.1169 | 1.32 | 9.96 |
| NADP | 744.0833 | 0.96 | 12.08 |
| CoA | 767.1152 | 3.78 | 10.02 |
| FAD | 785.1571 | 4.07 | 7.81 |
| Acetyl-CoA | 809.1258 | 5.05 | 8.98 |

**Table S-8 Growth of ADP1 wild type and mutant cells on different media**

| Strain | Medium used for growth | | |
|---|---|---|---|
| | succinate + shikimate | succinate | quinate |
| Wild type | + | + | + |
| Δ3353 | + | - | + |
| Δ1738 | + | - | + |

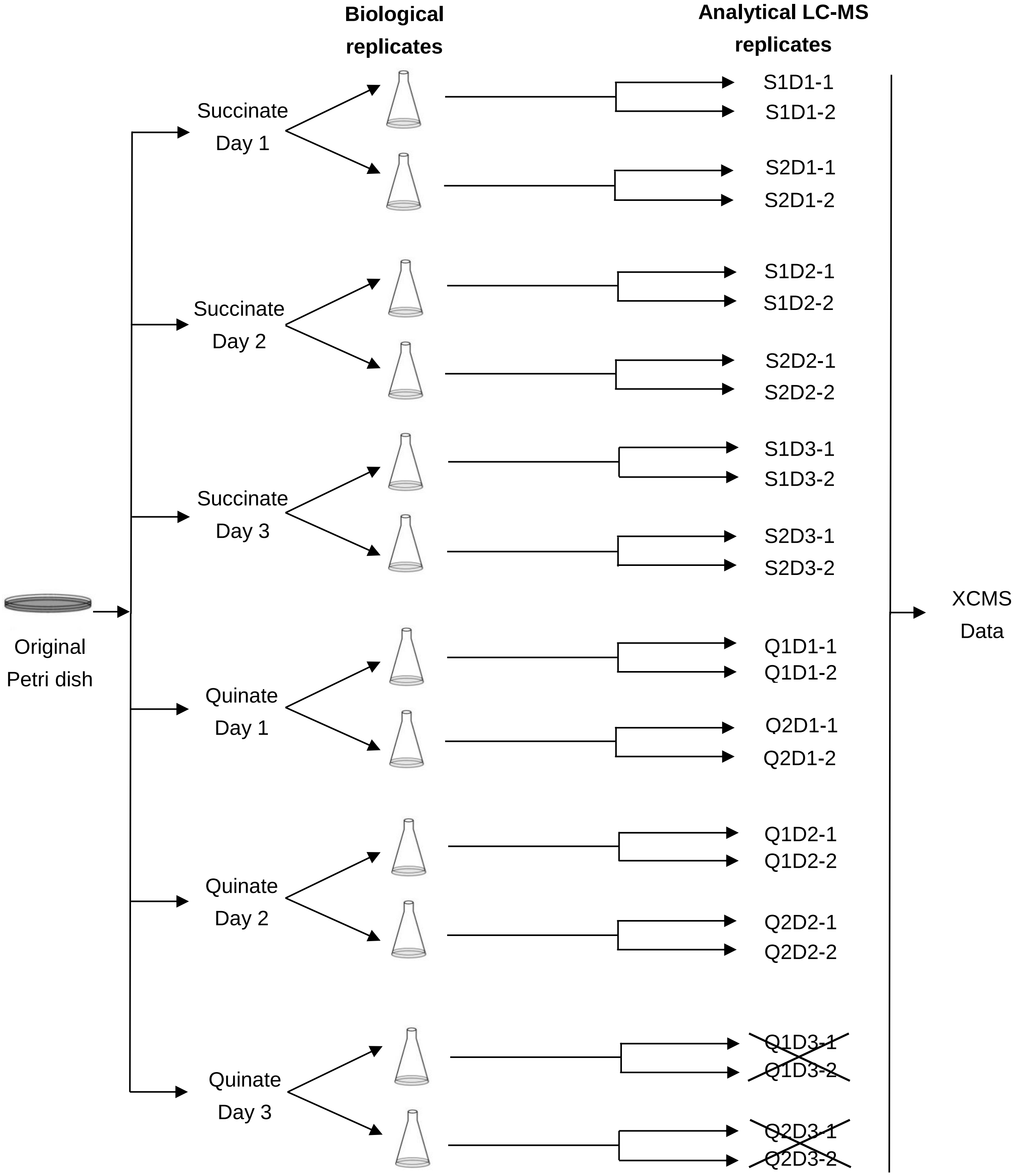


**Figure S-1 Metabolomic experimental design -** Experiments were conducted during 3 days; **c**ultures were performed in duplicates for each carbon source and the samples were analyzed in duplicate by LC-MS. Samples Q1D3-1, Q1D3-2, Q2D3-1, and Q2D3-2 were not taken into account.

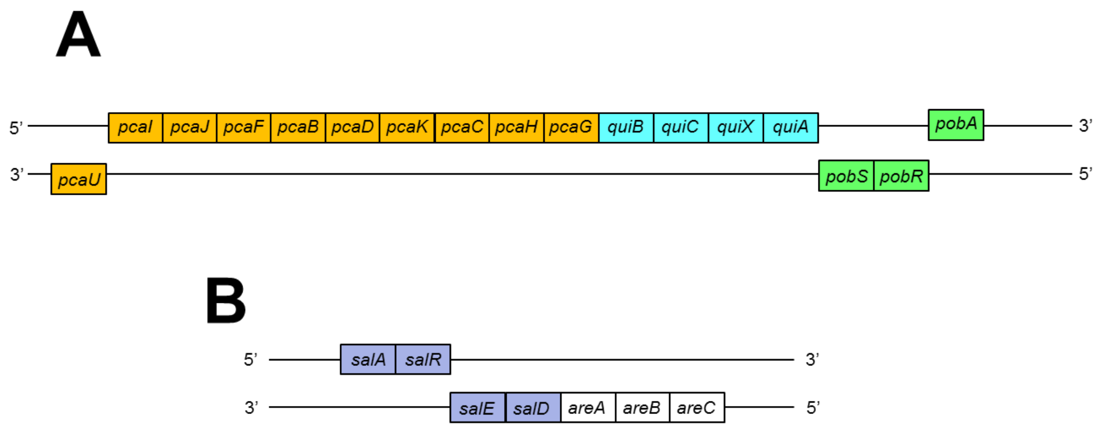


**Figure S-2** Chromosomal organization of genes involved in the metabolism of aromatic compounds. A: the *pca-qui-pob* cluster (protocatechuate branch). B: the *sal-are* cluster (catechol branch).

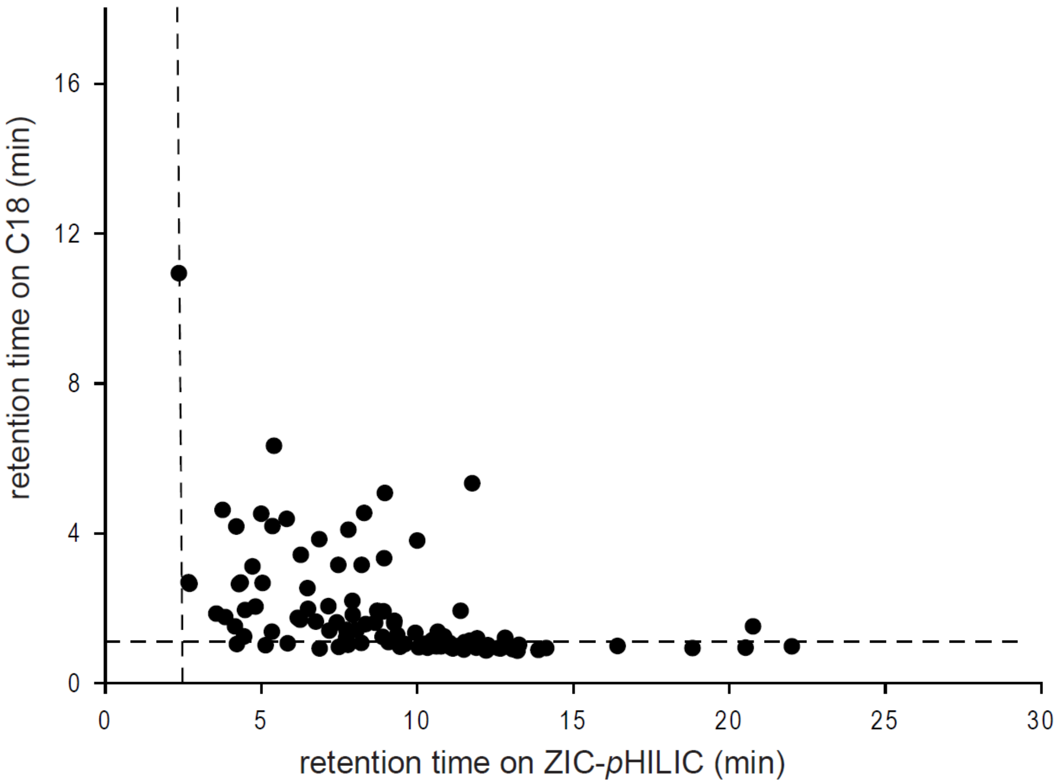


**Figure S-3 Retention times for 114 detected commercial compounds representative of the bacterial metabolism on the C18 and ZIC-pHILIC column** (see also Supplemental Table 5). The dotted lines represent the dead volume of each chromatographic column.

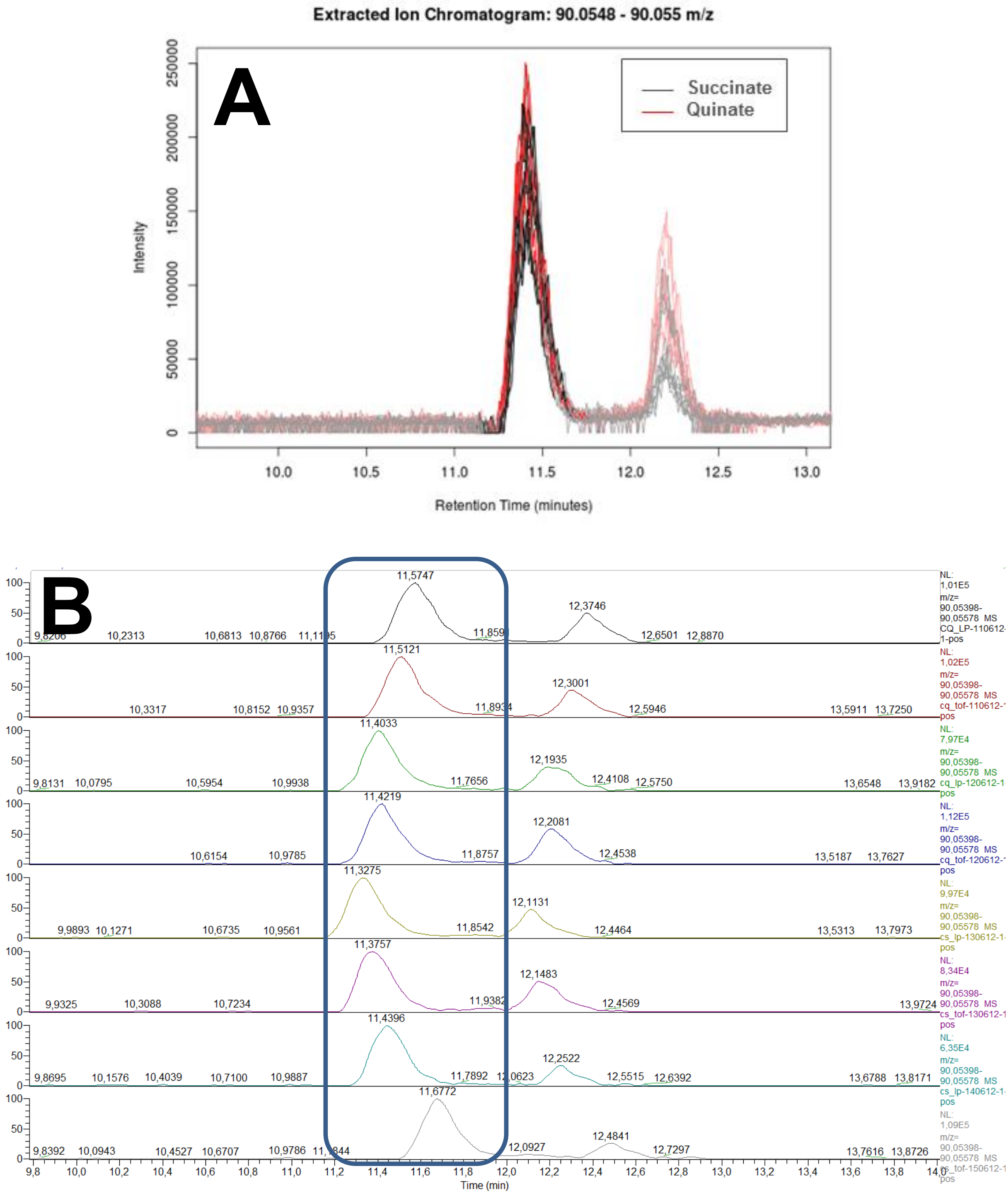


**Figure S-4 Quality of XCMS data processing (peak detection, retention time alignment and fold-change) for alanine (M90T682).** A: Extracted ion chromatograms from XCMS. B: Extracted ion chromatograms from RAW files. The four upper chromatograms correspond to files from the quinate group and the four bottom chromatograms correspond to files from the succinate group. Fold-change calculated by XCMS: 1.18. Fold-change calculated from peak integration in all the RAW files: 1.14.

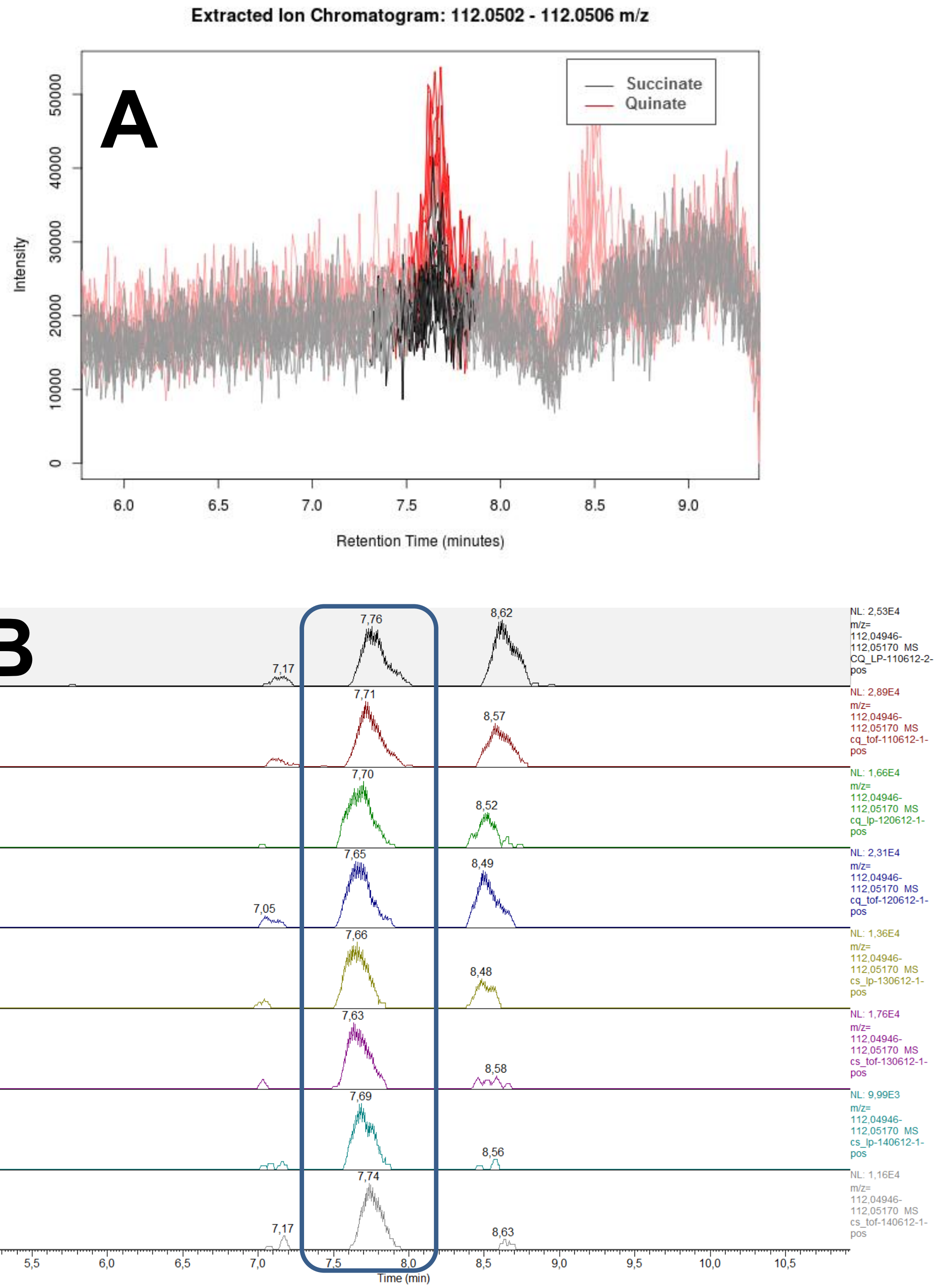


**Figure S-5 Quality of XCMS data processing (peak detection, retention time alignment and fold-change) for cytosine (M112T459).** A: Extracted ion chromatograms from XCMS. B: Extracted ion chromatograms from RAW files. The four upper chromatograms correspond to files from the quinate group and the four bottom chromatograms correspond to files from the succinate group. Fold-change calculated by XCMS: 1.71. Fold-change calculated from peak integration in all the RAW files: 1.62.

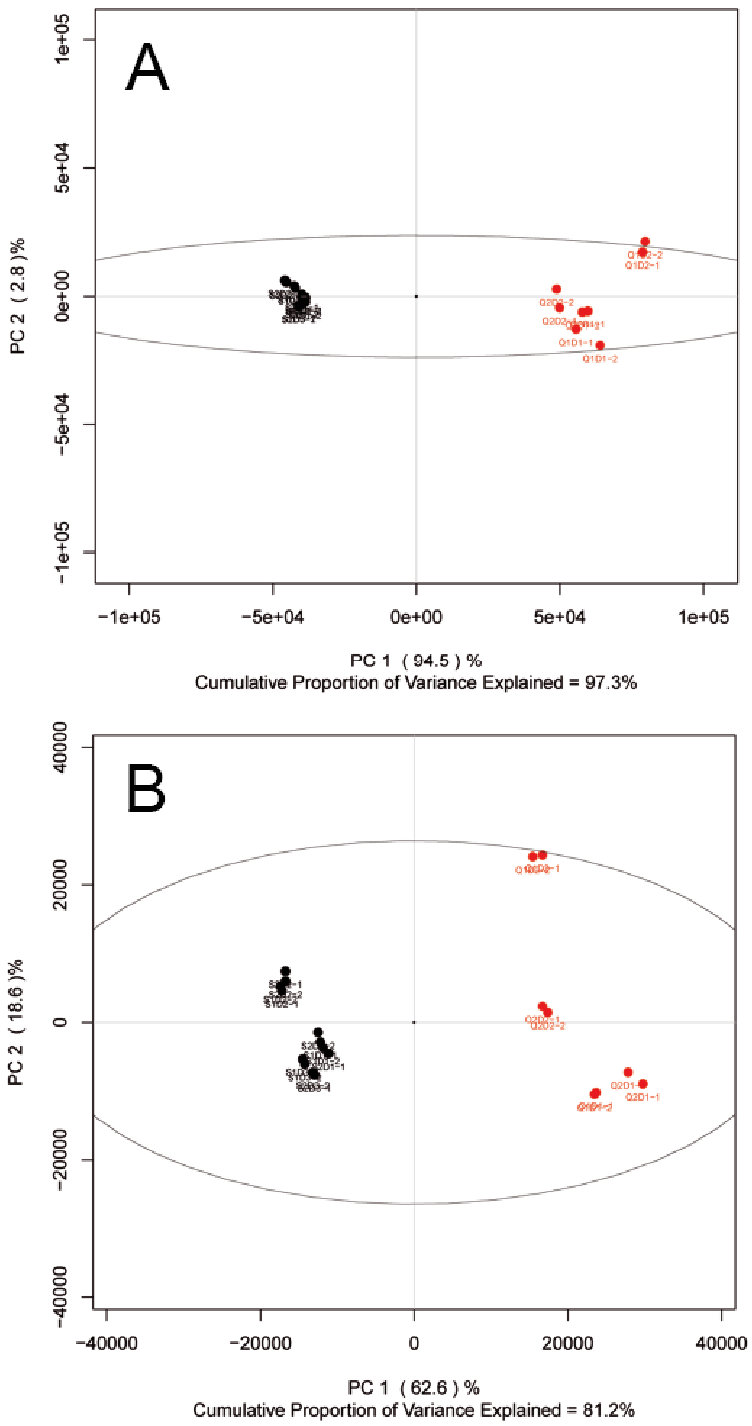


**Figure S-6 PCA scores plot of the effect of the carbon source change on the metabolome of Acinetobacter baylyi ADP1**. Metabolic fingerprints of ADP1 grown on succinate or quinate were recorded in negative (A) and positive (B) ionization modes. Data were mean centered and scaled to Pareto variance before multivariate statistical analysis. Quinate and succinate samples were represented by red and black circles, respectively.

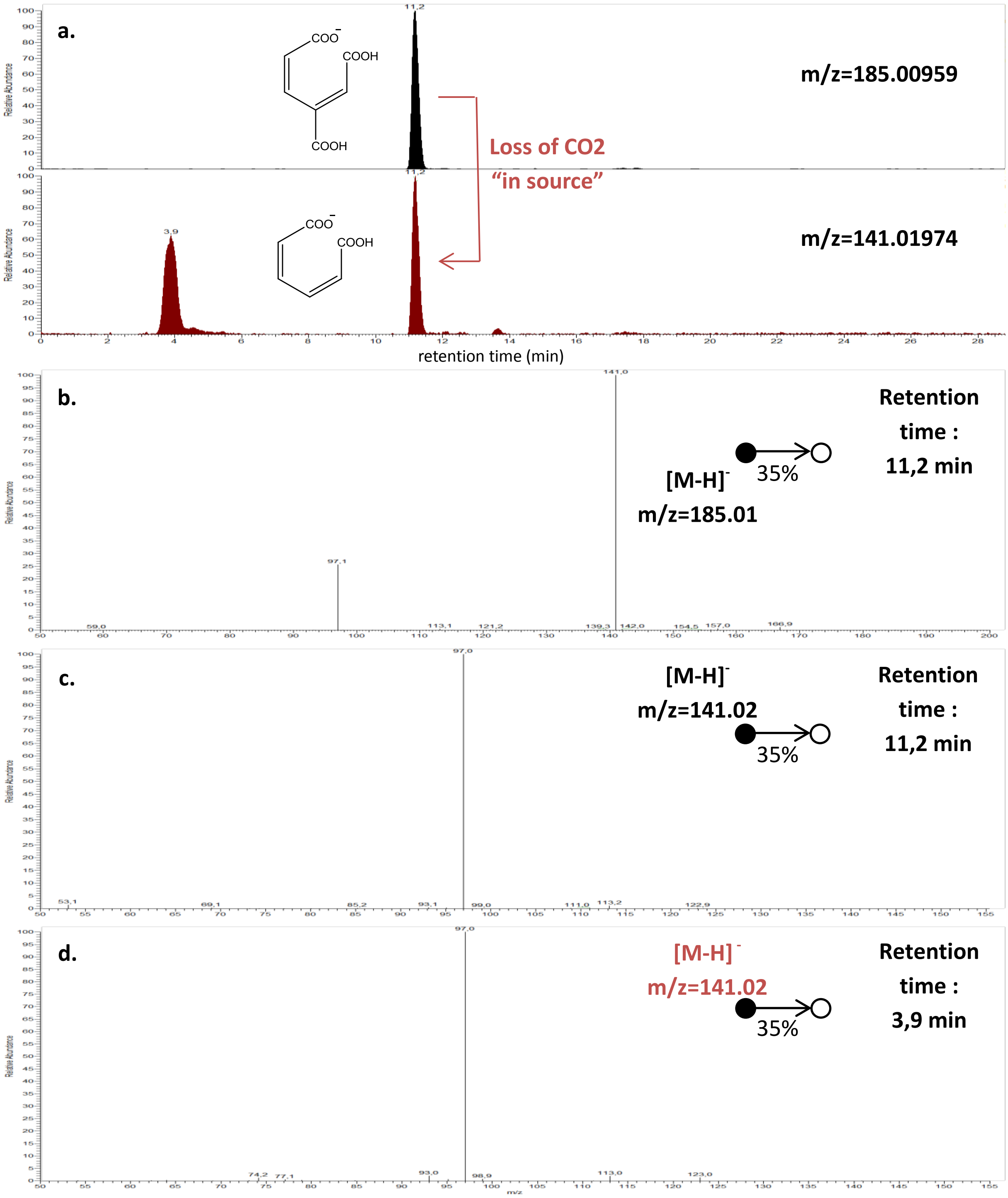


**Figure S-7 Extracted ion chromatograms (XIC) and tandem mass spectra for putative 3-carboxy-cis,cis-muconic acid (expected in ADP1) and cis,cis-muconic acid (not expected in ADP1) in negative ionization mode in biological samples**. **a.** XIC at the mass of 3-carboxy-cis,cis-muconic acid (185.00959) and at the mass of cis,cis-muconic acid (141.01974). **b.** $MS^2$ spectra from m/z 185,01 at 11,2 min. **c.** $MS^2$ spectra from m/z 141.02 at 11,2 min. **d.** $MS^2$ spectra from m/z 141.02 at 3,9 min.

At 11,2 min we observed (a.) the in-source fragmentation of the 3-carboxy-cis,cis-muconic acid in cis,cis-muconic acid (same retention time and chromatographic shape). We noticed that the $MS^2$ spectrum from the in-source cis,cis-muconic acid fragment (c.) was identical to the one from the peak with the same accurate mass at 3,9 min (d.). This suggested that the peak at 3,9 min was cis,cis-muconic acid.

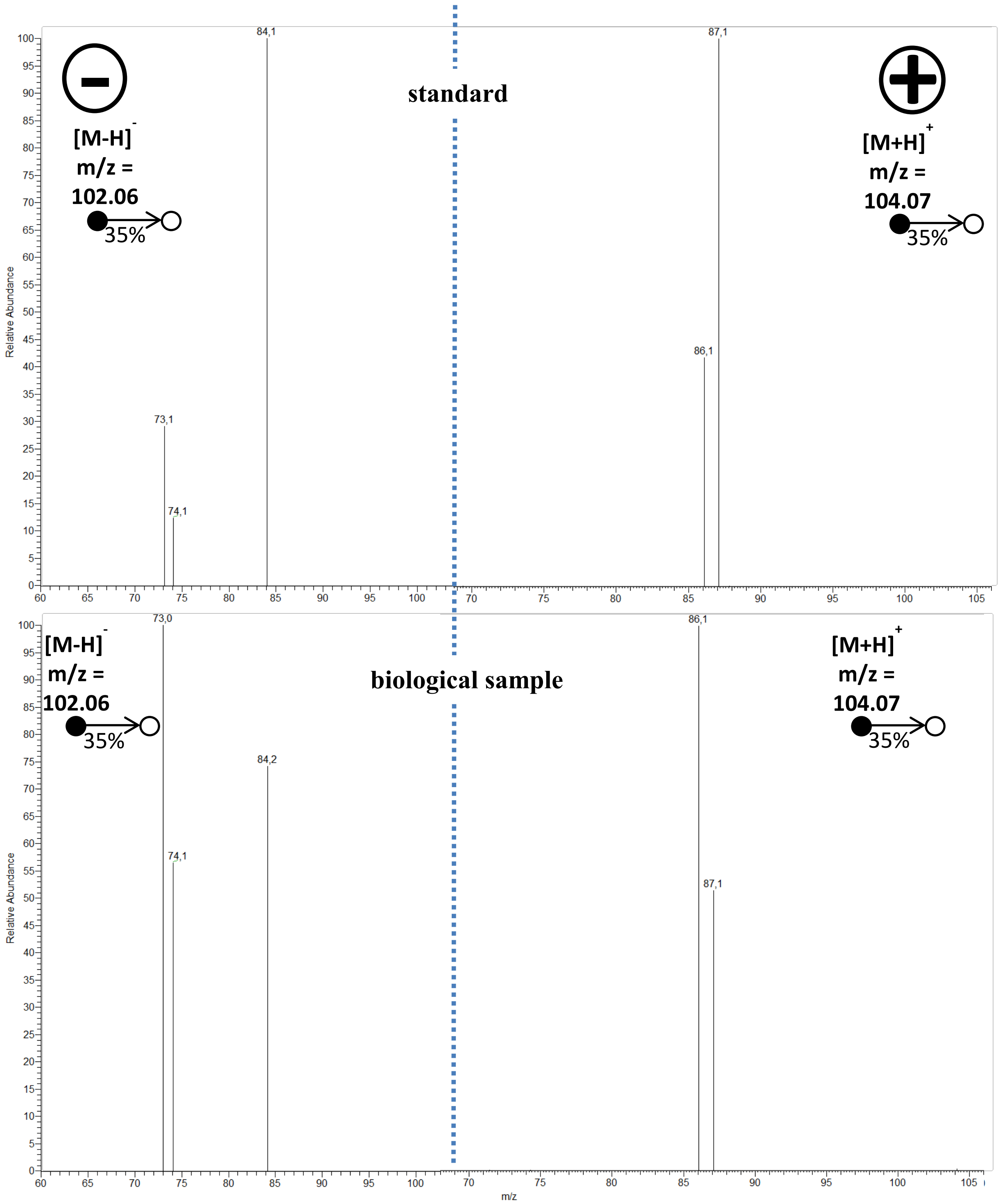


**Figure S-8 Tandem mass spectrum for GABA in negative ionization mode (-) and positive ionization mode (+).** The mass fragments of the reference compound were identical to those found in the biological metabolite, with slightly different relative intensities. These data were thus compatible with the presence of GABA in ADP1 metabolome.

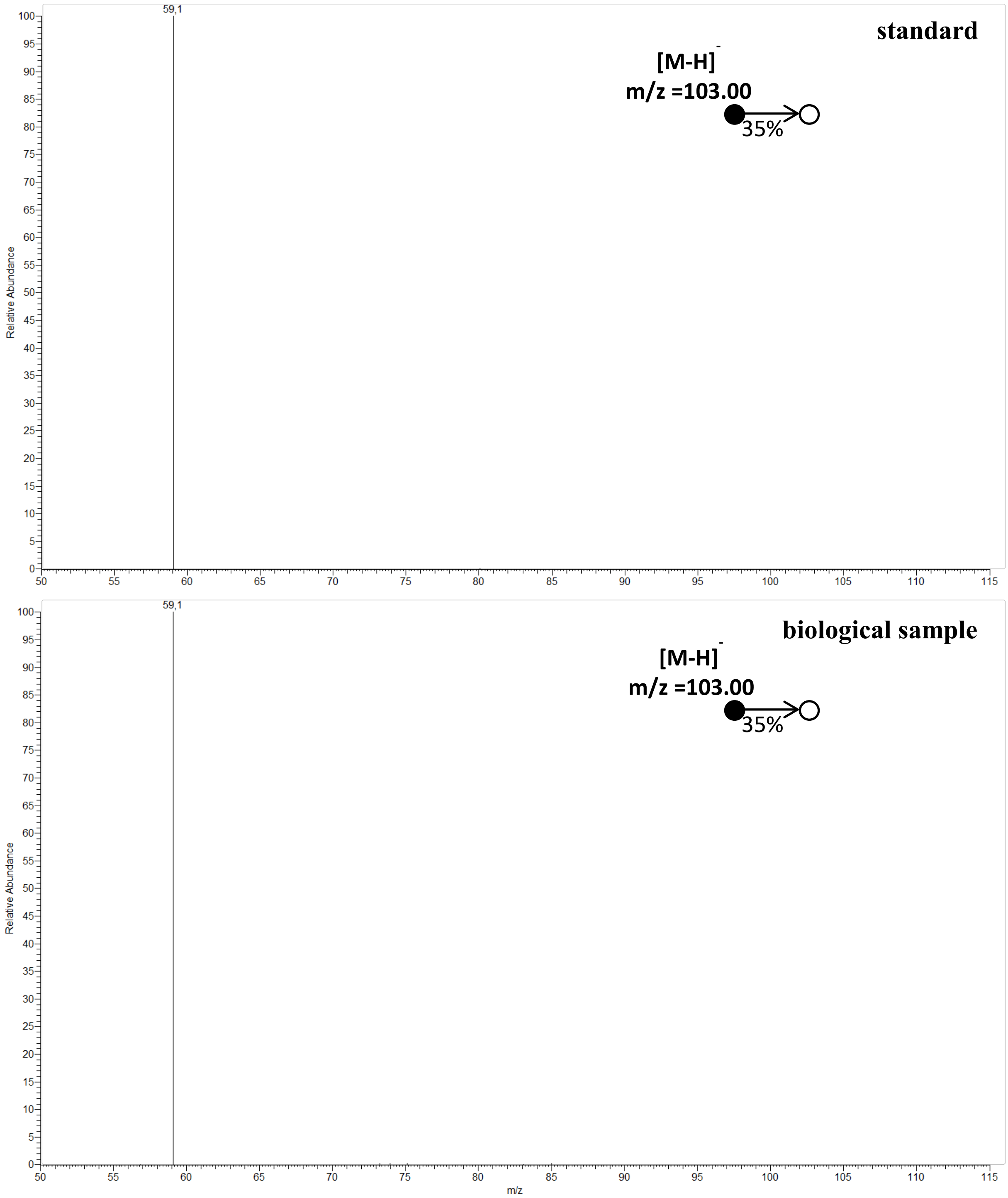


**Figure S-9 Tandem mass spectrum for malonic acid in negative ionization mode**. The mass of the fragment and its relative intensity were identical for the reference compound and the biological sample. These data were thus consistent with the presence of malonic acid in ADP1 metabolome.

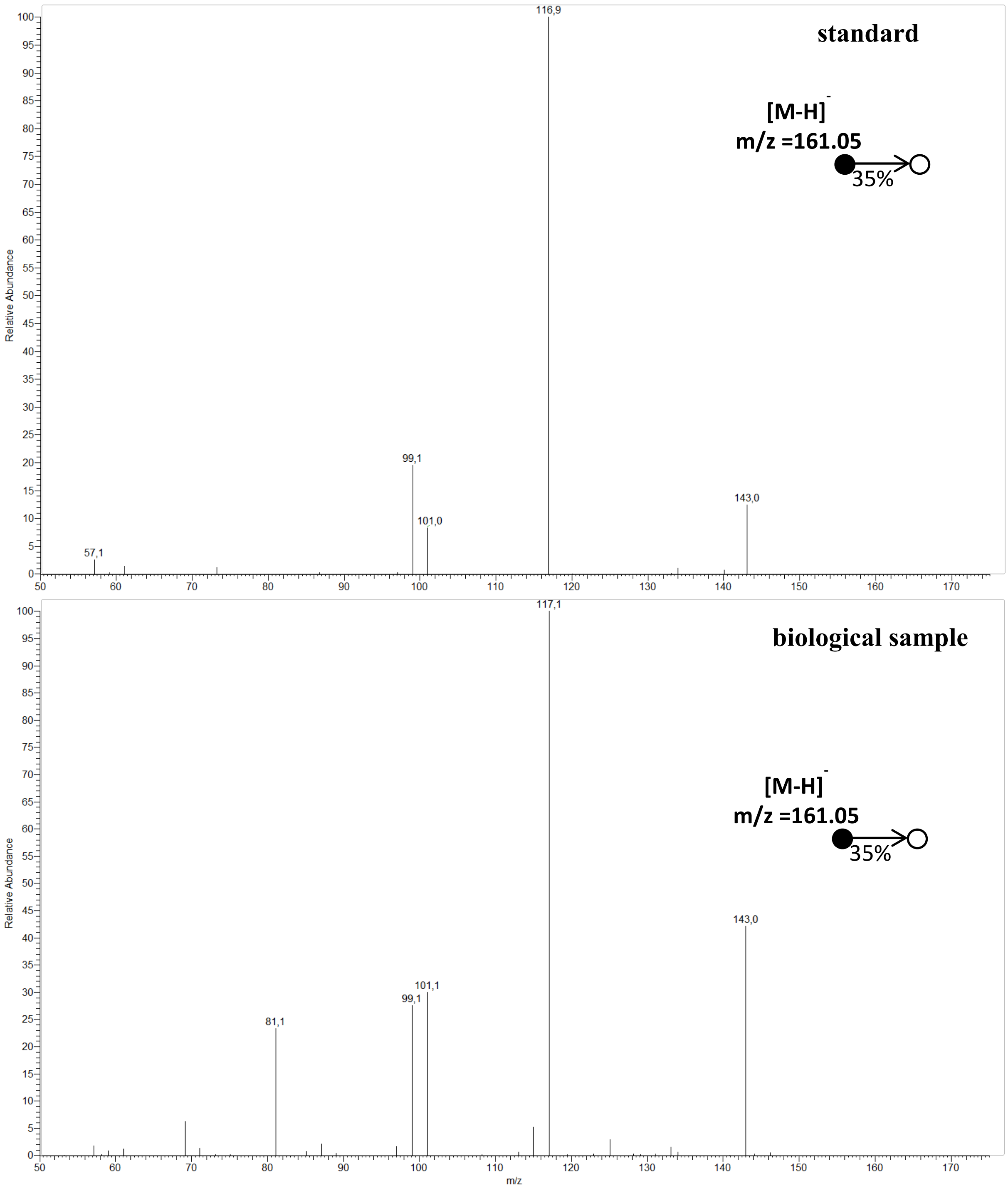


**Figure S-10 Tandem mass spectrum for 3-hydroxy-3-methylglutaric acid in negative ionization mode**. The fragments of the reference compounds were identified in the mass spectrum, with similar relative intensities. These data were thus consistent with the presence of 3-hydroxy-3-methylglutaric acid in ADP1 metabolome.

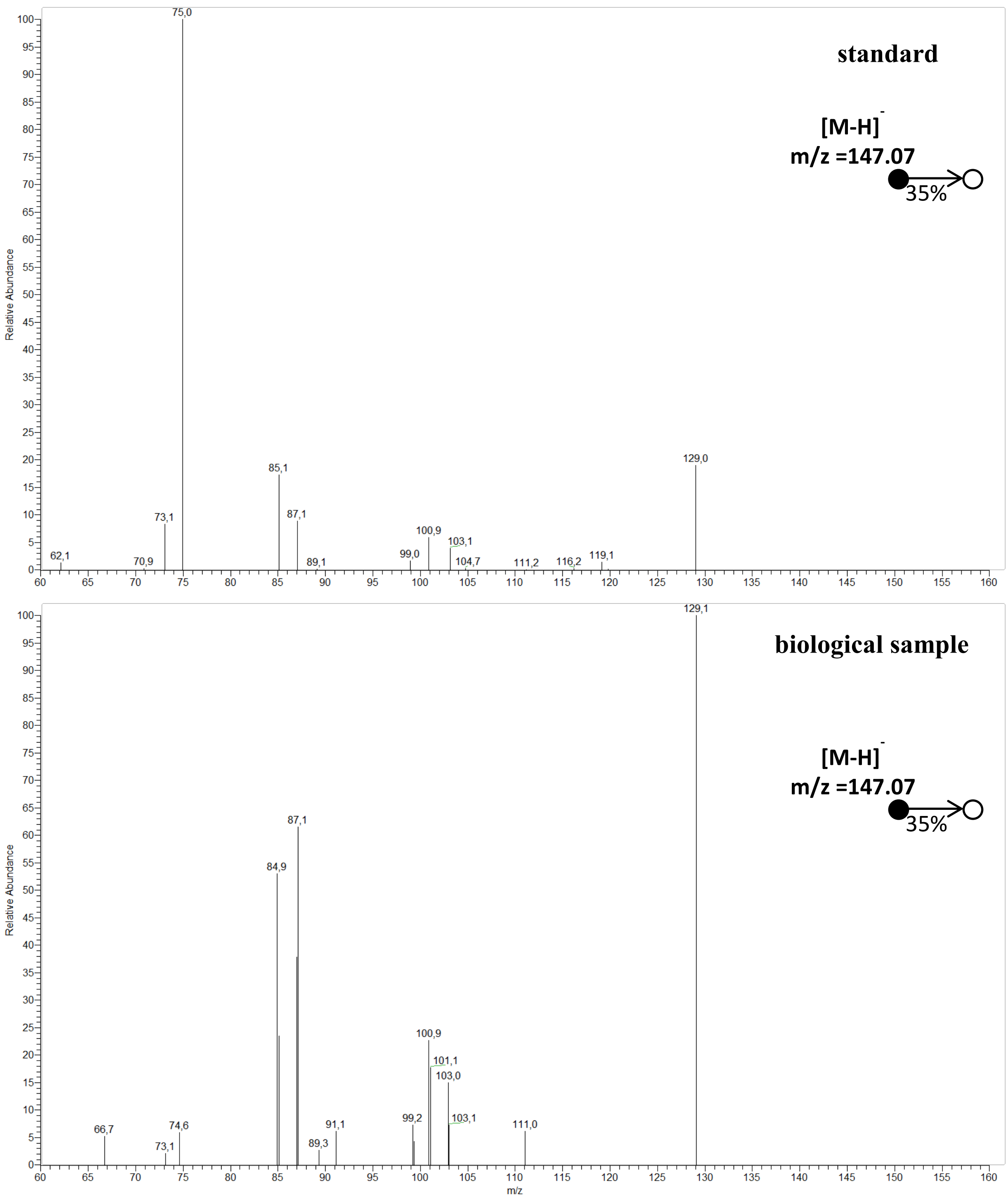


**Figure S-11 Tandem mass spectrum for mevalonic acid in negative ionization mode**. The main fragments of the reference compound were identified in the mass spectrum of the biological compound with slightly different relative intensities. These data were compatible with the presence of mevalonic acid in ADP1 metabolome.

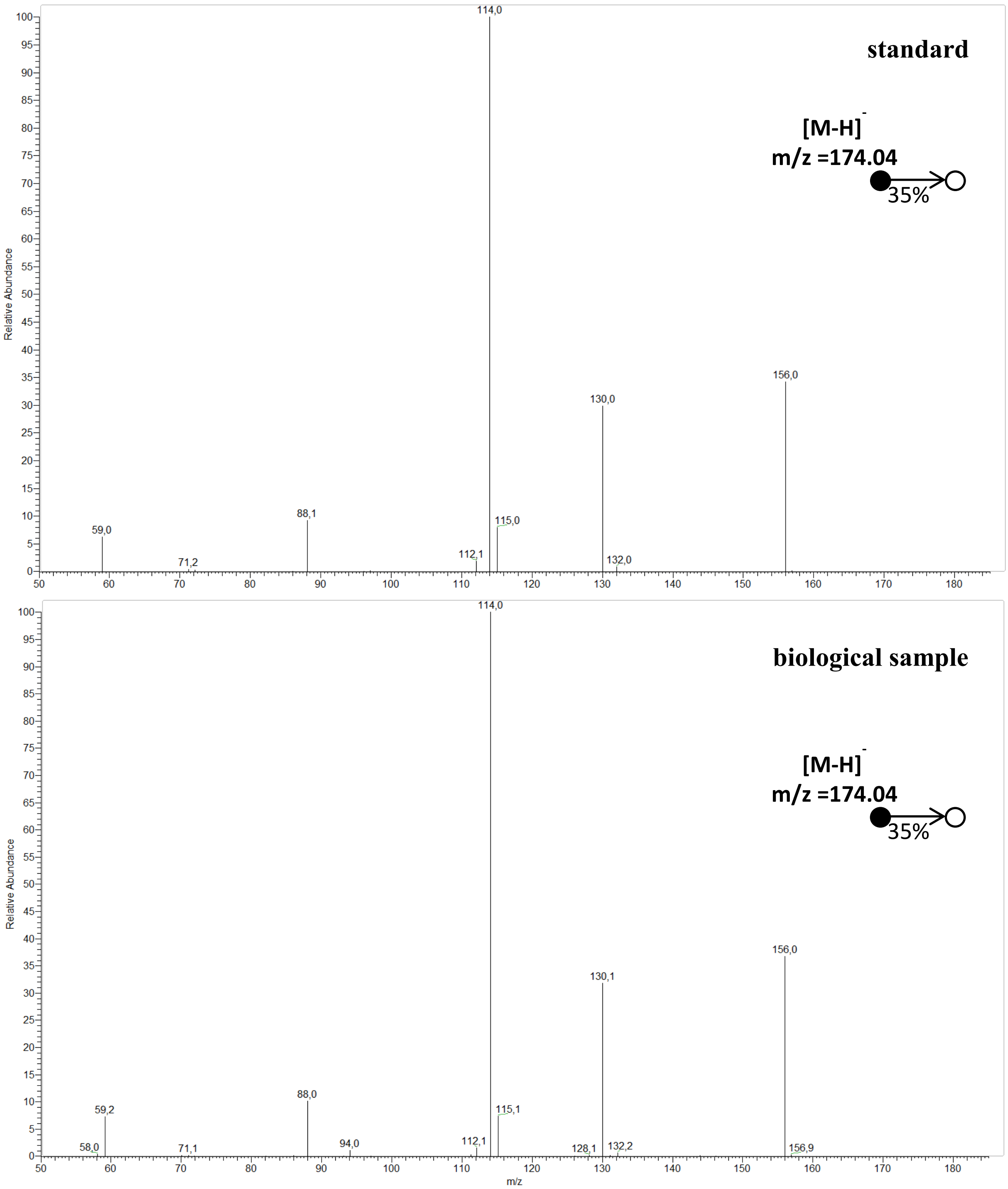


**Figure S-12 Tandem mass spectrum for N-acetyl aspartic acid in negative ionization mode**. The mass fragments and their relative intensities were identical in both the reference compound and the biological metabolite, suggesting the of N-acetyl aspartic acid in ADP1 metabolome.

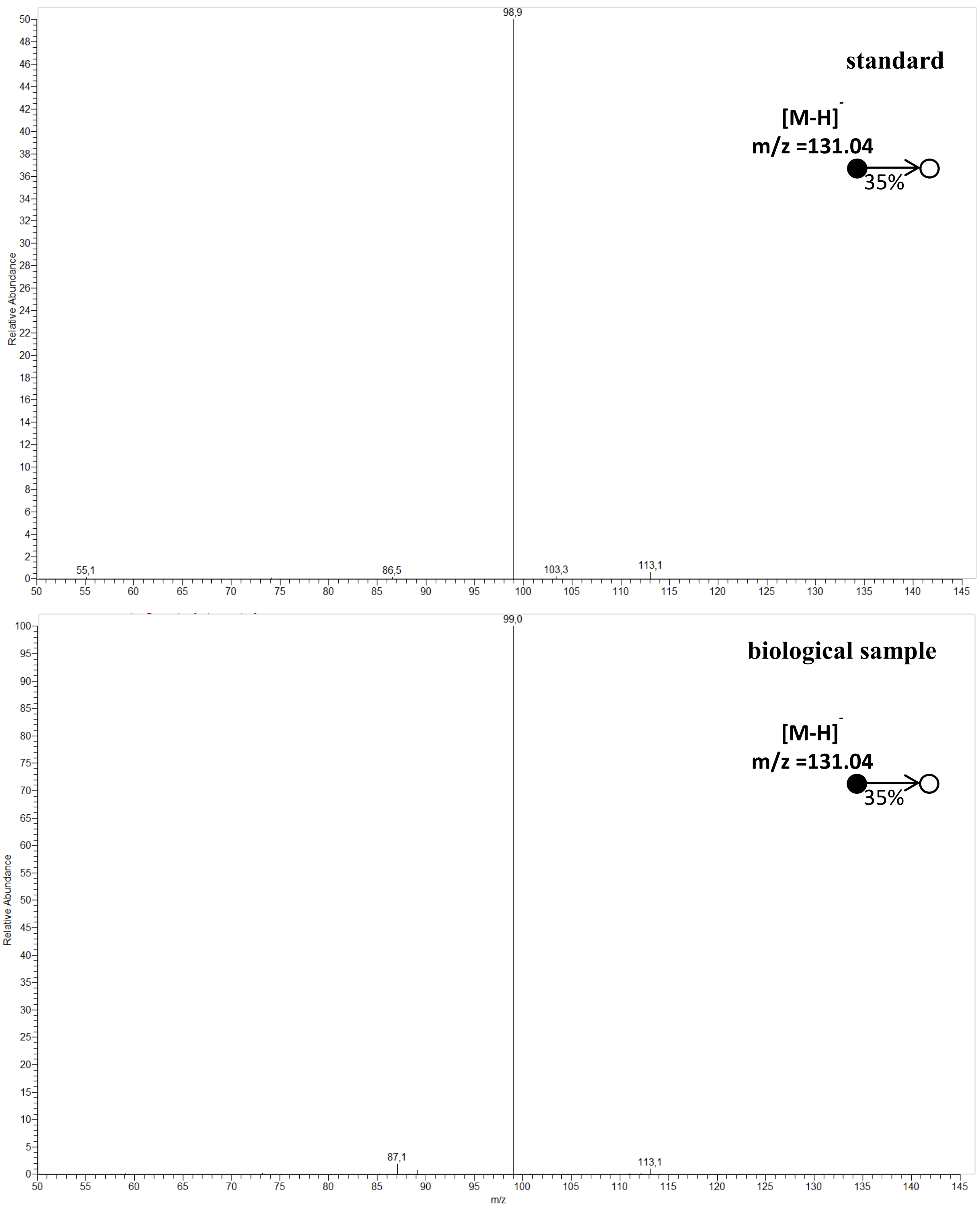


**Figure S-13 Tandem mass spectrum for mono-methyl hydrogen succinic acid in negative ionization mode**. The main fragments of the reference compound were identified in the mass spectrum of the biological metabolite, with identical relative intensities. These data were compatible with the presence of

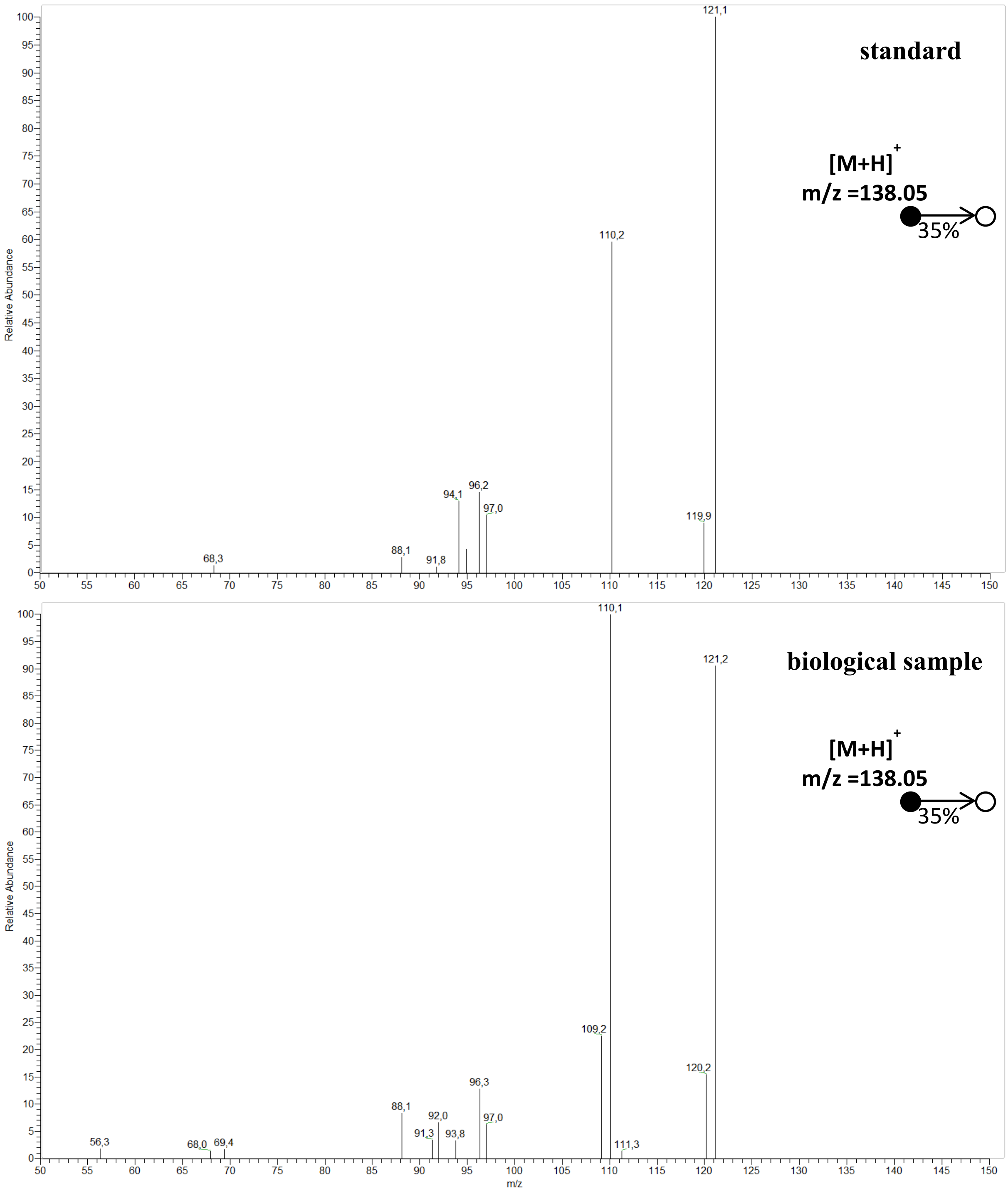


**Figure S-14 Tandem mass spectrum for trigonelline in positive ionization mode**. The fragments of the reference compound were identified in the mass spectrum of the biological metabolite, with identical relative intensities. These data were compatible with the presence of trigonelline in ADP1 metabolome.